A Beam Spreader System for LCLS-II*

T. Beukers†, J. Amann, Y. Nosochkov, SLAC National Accelerator Laboratory, Menlo Park, USA

Abstract

For the LCLS-II project, the SLAC National Accelerator Laboratory is installing a new superconducting RF linac capable of continuously delivering 4 GeV electron bunches spaced 1.1 microseconds apart. A spreader system is required to distribute the beam between a soft X-ray or hard X-ray undulator, and a beam dump. An additional beam diverter is required in the front end of the linac to divert 100 MeV electrons to a diagnostic line. Both the spreader and diagnostic diversion systems are designed to operate on a bunch by bunch basis via the combination of fast kickers and a Lambertson septum. This paper presents a summary of the beam transport, kicker, and septum design. Of specific interest is the unique challenge associated with building a high repetition, high stability spreader capable of diverting a single bunch without disturbing neighbouring bunches. Additional discussion includes the application of the spreader technology to the proposed S30XL beamline. This beamline will accept micro bunches evenly spaced between the undulator bound bunches, thus requiring a kicker with the same repetition rate as LCLS-II but a pulse width extended to approximately 600 ns.

INTRODUCTION

The LCLS-II [1] free electron laser (FEL) project at the SLAC National Accelerator Laboratory will produce 4 GeV electron bunches from a superconducting linac (SRF) at a repetition rate of 929 kHz. These bunches will be steered via a spreader to a hard X-ray (HXR) undulator, a soft X-ray (SXR) undulator, or an electron beam dump in the Beam Switch Yard (BSY). Each undulator requires a dedicated beam diverter consisting of three kickers and a septum. The kickers are pulsed simultaneously to produce an integrated kick sufficient to direct each bunch into the high field region of a septum magnet where the bunch is steered towards the corresponding undulator. When neither set of kickers is pulsed, the beam traverses the zero-field region of both septa and is transported to the BSY dump. This spreader design has the capability to produce semi-arbitrary bunch-by-bunch beam patterns between the two undulators and the BSY dump. Primary components of the spreader have been designed, built, and tested, including the kickers and septa. Discussion will include beam transport through the spreader, kicker design and testing results, modification of the kicker design for high strength or long pulse applications, and septum design.

BEAM TRANSPORT

After the SRF linac, the 4 GeV beam is transported via a dogleg and existing 2-km bypass line to the beam spreader system located at the end of the existing LCLS [2] CuRF linac and in the BSY. The spreader fast vertical kickers and horizontal septa divert the SRF bunches either to HXR or SXR undulator beamlines or allow them to pass to the 250 kW dump in the BSY muon wall. The 3 – 17 GeV bunches from the CuRF linac are also diverted in this region to the HXR or SXR or to the existing End Station-A beamline (ESA) using low repetition kickers. Consequently, several beamlines occupy less than 1 m^2 cross-section in this area.

The spreader layout is shown in Fig. 1, where the fast kickers and septa (in dash boxes) divert the SRF beam to HXR and SXR beamlines (green and light blue), to BSY dump (black box), or to ESA through S30XL (red). The CuRF beam is diverted to the HXR, SXR or ESA. The different beamlines are at different elevation level.

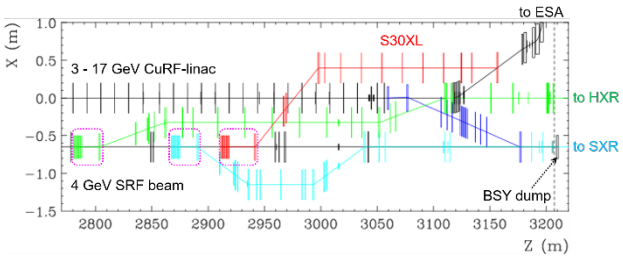

Figure 1: Top view of the spreader.

The SRF beam pattern consists of the primary FEL bunches spaced 1.1 μs apart, intended for the undulators, and the dark current buckets between them which are populated at the LCLS-II RF gun (with 5.4 ns spacing) or may be seeded by a 46-MHz laser oscillator (21.5 ns spacing). The first fast kickers on the SRF beam path are for the HXR (see Fig. 1). When these kickers' pulse is on, the FEL bunches are deflected through the HXR septum high-field hole into the HXR beamline; otherwise they proceed straight ahead through a field-free hole towards the SXR kickers and septum. Similarly, if the SXR kickers' pulse is on, the FEL bunches are deflected into the SXR beamline; otherwise they pass towards the BSY dump. The 4 GeV LCLS-II uses three fast kickers for each undulator, while for the future LCLS-II high energy upgrade (8 GeV) the number of kickers will be increased to six.

Due to the short kicker pulse, the dark current between the FEL bunches is not affected by the HXR and SXR kickers and nominally goes to the BSY dump. Lately a new beamline, named sector 30 transfer line (S30XL – red line in Fig. 1), formerly DASEL [3], has been proposed which would divert the dark current or seeded low charge bunches to the ESA facility for dark matter experiments [4] using a long-pulse vertical kicker and the HXR/SXR type septum, where the kicker pulse is shaped to deflect only the ~600 ns of the dark current between the FEL bunches. The S30XL operates parasitically to the FEL because the dark current

*Work supported by Department of Energy contract DE-AC02-76SF00515.
† beukers@slac.stanford.edu.

has a very low charge and is deflected downstream of the HXR/SXR kickers. Six S30XL kickers are planned to be used, sufficient for up to 8 GeV beam energy.

KICKER

Design

The detailed electrical design of the kicker system is presented in [5] and summarized here in addition to updated test results from the as-built system. For 4 GeV beam, the spreader kicker's design specification requires a 12 mT-m pulsed integrated field with rise and fall times short enough to accommodate the 1.1 µs spacing between bunches. To avoid radiation damage and decrease MTTR the kicker electronics are located outside of the tunnel. To prevent long inductive switching times and reflections, a transmission line system design, with matched cabling, kicker magnet, and load is utilized. For ~1 MHz switching, discrete MOSFETs are a well-suited choice. However, they are limited in operation to the ~1 kV range, too low to provide an effective electric field kick. Thus, a magnetic ferrite loaded lumped element transmission line kicker topology was selected.

To achieve the required integrated field, three 1 m long kicker magnets, each providing 4 mT-m, are pulsed simultaneously. Each kicker section is composed of 18 gapped ferrite blocks arranged to enclose a ceramic beampipe as shown in Fig. 2.

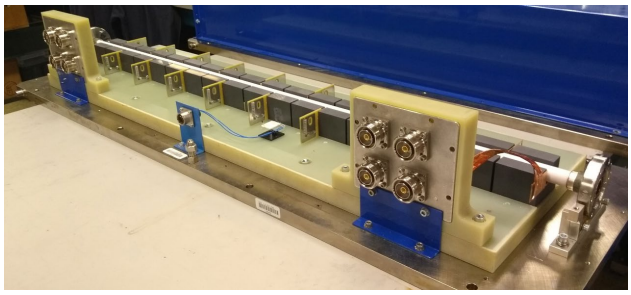

Figure 2: Kicker magnet with cover and top busbar removed.

The ceramic beampipe provides UHV isolation. The 10 mm ID of the beampipe is coated with a conductive layer of titanium to prevent charge build-up. Beneath the beampipe, a supply current busbar runs the length of the magnet. A second busbar is installed on the top side of the magnet to provide a return current path. Between each ferrite section a capacitor is installed between the supply and return busbar. When combined with each ferrite's inductance a characteristic transmission line impedance, Z, is formed.

The pulse is terminated into a matched resistive load. The fill-time of the structure, τ, is given by:

$$\tau = L_T/Z,$$

where L_T is the sum of each ferrite's inductance, dominated by the magnetic energy stored in the volume of the gap which has a square cross section with a width of 20 mm. The impedance was selected to be low enough such that the 900 V peak pulser voltage can produce adequate current for the required field. However, the impedance must remain high to limit fill-time. A 12.5 Ω impedance was selected, yielding an idealized fill-time of 101 ns. In practice, the fill-time is increased to ~125 ns due to the rise-time of the voltage pulse and the cut-off frequency of the magnet's ferrite-capacitor cells. Between pulses the magnet must fill and empty yielding a ~250 ns time period for which there is magnetic field in the structure.

Given the extremely high rate, components were carefully selected to limit power dissipation within the magnet. The ferrites are composed of Ferroxcube's 4M2 NiZn soft ferrite, where losses are calculated to be only 9 W/m at 929 kHz operation [5]. Chip mount C0G style capacitors soldered in parallel on PCBs make-up the cell capacitance which can be easily tuned by the addition or subtraction of capacitors.

The pulse driver is composed of a large filter capacitor feeding 4 parallel 1.2 kV MOSFETs. To prevent overvoltage, an extremely low inductance current path is maintained and the switches are limited to 900 V operation. Four parallel 20 m, 50 Ω cables are used to connect the driver to the magnet. To prevent a long pulse tail caused by magnet dispersion, large 7/8" Heliax are used. The terminating load is composed of parallel water-cooled thick film resistors overrated to absorb the 5.5 kW produced from 929 kHz pulse generation.

Test Results

Measurements of the prototype kicker system were presented in [5]. For the final kicker system several modifications were made. Holes were machined in the base of the ferrite blocks to improve mounting. Rather than the load being directly connected to the magnet, 2 m of matched impedance cabling was added. Finally, the grounding of the cable termination to the magnet was improved. The updated measurements are presented.

In order to not perturb the bunch following the kicked bunch it is essential that the remaining magnetic field ringing in the structure rapidly decays. This can most accurately be measured by measuring the voltage across the capacitor of every cell. The ringing voltage in the capacitors is proportional to the ringing magnetic field in the cell gap. The remnant field is presented as the ratio of the sum of voltages ringing in all 18 cells at a given time following the peak of the integrated field vs the sum of voltage when the integrated field is at peak amplitude. At 1.1 µs following the peak pulse, the field ringing envelope has decayed to 131 ppm of the main pulse. By 2.2 µs, the remnant field has decayed to less than the 60 ppm required to meet specification.

To measure the stability of the pulse, the load voltage was measured over several thousand non-consecutive pulses. The calculated standard deviation is 101 ppm. Additionally, taking into account the random noise of three separate kickers, the stability is improved by a factor of 1.7.

Bdot measurements were integrated to measure the transverse field quality. Four measurements were made with horizontal and vertical offsets 1 mm from the center of the magnet. In the worst case, the variation from the center was 0.21%. Reliable operation at 500 kHz has been demonstrated.

Application to Diagnostic and S30XL Line

An additional LCLS-II diverter system is composed of one kicker and one septum to steer 100 Hz of 100 MeV beam into a diagnostic line at the front end of the accelerator. To accommodate a larger stay clear, the width of the ferrite cross section is increased by 75%. Because the ferrite gap is square, the inductance remains constant. However, the current and voltage increase to accommodate the increased gap. To generate the required 3.1 mT, a pulser with a peak voltage of 1.4 kV was built.

The S30XL line requires a much different set of kicker parameters. This kicker system, still under development, will kick continuous very low charge bunches spaced between the 929 kHz LCLS-II bunches into the S30XL line. Thus the kicker is required to have a high duty cycle, only turning off to let LCLS-II bunches destined for the beam dump to pass through unperturbed. The kicker will operate at 929 kHz with an initial 525 ns flat-top (possibly extendable to 600 ns). An integrated field of 18 mT-m (including 20% overhead) is required to be compatible with the 8 GeV LCLS-II upgrade. To meet this requirement, 6 kicker magnets running at 75% of the nominal spreader amplitude are required. Additionally, since the dump bound beam is less sensitive to remnant field in the kicker, the pulse width can be extended and two kicker magnets can be filled in series from a single driver and terminated into a single load. The higher duty cycle operation increases the average driver output and absorbed load power by a factor of 3.8 which can be accommodated by paralleling more driver transistors and load resistors.

SEPTUM

Design

The spreader septum is a Lambertson type septum magnet, with a circular profile field free region and a 3" wide pole. Due to the 15 mm maximum separation of the kicked and un-kicked beams leaving little space for a vacuum chamber, the spreader septum requires an in-vacuum pole. The spreader septum has engineering name 0.625SD38.98, having a dipole gap of 0.625" and a core length of 38.98". A picture of the septum is seen in Fig. 3. The design parameters for the 0.625SD38.98, sufficient for up to 10 GeV of the HXR and SXR beams, are given in Table 1.

Figure 3: Spreader septum.

Table 1: Design Parameters for 0.625SD39.38 Lambertson Septum Magnet

Parameter	Value	Units
Max. Integrated Field	3.689	kG-m
Trim Coil Range	+/- 2	%
Max. Quadrupole Field @ r = 5 mm	<0.05	%
Max. Sextupole Field @ r = 5 mm	<0.2	%
Max. Decapole Field @ r = 5 mm	<1	%
Magnet Gap	0.625	inches
Effective Length	1.03	m
Main Coil Max. Current	124	A
# of Main Coil Turns	45	turns
Trim Coil Max. Current	6	A
# of Trim Coil Turns	20	turns

Vacuum Enclosure Construction

The lower pole containing the field free region and the dipole gap region is partially enclosed by a vacuum chamber which is welded TIG directly to the C1006 steel. In order to meet UHV vacuum outgassing requirements, the C1006 steel pole has an electroless NiB plating applied prior to welding of the vacuum chamber. The choice of NiB electroless plating is due to the highly uniform deposit of NiB alloy which additionally lacks the undesirable ferromagnetic properties of electroplated Ni.

Manufacturing Status

Currently, the spreader septa are completing manufacturing at SLAC. The coils have been manufactured and delivered by a magnet vendor. The core machining is complete at the SLAC machine shops and the lower core pieces have been NiB plated. Magnetic measurements has been completed by the SLAC metrology group and final assembly is underway. One unit, shown in Fig. 3, has been completed and tested.

REFERENCES

[1] T.O. Raubenheimer, ``LCLS-II: status of the CW X-ray FEL upgrade to the SLAC LCLS facility'', in *Proc. 37th International Free Electron Laser Conference (FEL'2015)*, Daejeon, Korea, Aug. 2015, paper WEP014, pp. 618-624.

[2] A P. Emma, et al., "First lasing and operation of an angstrom-wavelength free-electron laser," Nature Photonics, vol. 4, p. 641-647, Aug. 2010.

[3] T. Raubenheimer *et al.*, "DASEL: Dark Sector Experiments at LCLS-II," SLAC-PUB-17225, arXiv:1801.07867 (2018).

[4] T. Nelson, "Light Dark Matter eXperiment: a missing momentum search for light dark matter," in *US Cosmic Visions: New Ideas in*

Dark Matter Workshop, University of Maryland, College Park, USA, Mar. 2017, https://indico.fnal.gov/conferenceDisplay.py?ovw=True&confId=13702

[5] T. Beukers, M. Nguyen, T. Tang, "Discrete Element Transmission Line Beam Spreader Kickers for LCLS-II," *2018 IEEE International Power Modulator and High Voltage Conference (IPMHVC)*, Jackson Lake Lodge, WY, 2018.